

Developing a Resilience-Based Optimization Framework for Life-Cycle Costing Infrastructure Management

Pedram Omidian ¹, Naser Khaji ^{2*}, Ali Akbar Aghakouchak ¹

1- Faculty of Civil and Environmental Engineering, Tarbiat Modares University, P.O. Box 14115-397, Tehran, Iran

2- Civil and Environmental Engineering Program, Graduate School of Advanced Science and Engineering,
Hiroshima University, 1-4-1, Kagamiyama, Higashi-Hiroshima, Hiroshima 739-8527, Japan

nkhaji@hiroshima-u.ac.jp

Abstract

Bridges as one of the most critical components of transportation infrastructure play an important role in providing essential services to communities. Therefore, preparing disaster management strategy is necessary by selecting reliable, robust, and efficient indicators. In this study, a multi-objective optimization framework is presented to identify the most optimal retrofit strategies which satisfying a given threshold of Resilience (R), while minimizing the corresponding Life-Cycle Cost (LCC) of an infrastructure against hazardous events during its life-cycle by employing the Non-dominated Sorting Genetic Algorithm II (NSGA-II). In each scenario, the fragility curves are derived by performing Incremental Dynamic Analysis (IDA) for evaluating the LCC and resilience. In the next step, the LCC analysis is conducted during the service lifetime that incorporates the effects of complete/incomplete repair actions of damage conditions induced by multi-occurrence of previous seismic hazard event. Results show that the considered objectives lead to reasonable and sense-making retrofit strategies.

Keyword: Infrastructures management; Life-cycle cost; Multiple occurrences; Resilience; Retrofit optimization framework

Introduction

One of the most critical functions of bridge infrastructure systems such as transportation networks is to provide essential services to communities and to support their economic growth, security, and competitiveness. Bridges are constantly exposed to different natural disasters during their life-cycle among which earthquakes can occur multiple times with different intensities. As a result, if an incurred damage is not fully repaired before the next hazardous event, it leads to the accumulation of damage and more seismic vulnerability [1]. Therefore, it is necessary to use the effective and dynamic decision-making frameworks that correctly model expected risks, dependencies and uncertainties in the form of sensible indicators. The total Life-Cycle Cost (LCC) is a logical and pragmatic monetary index in which includes initial construction costs, maintenance costs, cost of possible retrofit measures, and repair costs [2]. In this respect, several studies have been accomplished on the development of the LCC frameworks to identify the optimal for managing infrastructure systems that are exposed to extreme natural disasters [3]. Zhu and Liu [4]

presented a maintenance strategy optimization framework for Reinforced Concrete (RC) girder bridges by considering four separate objective functions including condition index, reliability index, service life, and life cycle maintenance cost by manipulating Non-dominated Sorting Genetic Algorithm (NSGA). Omidian and Khaji [5] proposed a multi objective optimization framework for seismic resilience improvement of RC structures by selecting the most optimal strategies that optimized for resilience index and the cost of retrofit using NSGA-II.

In the field of infrastructure management, proposing a decision-making methodology is becoming a high-priority demand for policy-makers in order to find optimal strategies for disaster risk reduction [6]. The aim of this research is to propose a sense-making optimization framework by investigating and comparing different objectives (i.e., the LCC and resilience index) in the form of multi-objective optimization, that provides a clear picture from the current and future states of the under-study infrastructure for decision-makers during its life-cycle. For this reason, a typical bridge is considered as a

case study infrastructure with different pier retrofit strategies including ten different times of retrofitting action, eight retrofitting arrangements, and two materials with four thicknesses (namely, Carbon Fiber Reinforced Polymer (CFRP) and Glass Fiber Reinforced Polymer (GFRP)). In the first step, a series of nonlinear time-history Incremental Dynamic Analysis (IDA) is performed to evaluate the fragility curves for each case, which are the basis for constructing the seismic resilience curves/surfaces. Following, the LCC are calculated based on hazard curve and fragility curves. In addition, a well-known fast and elitist multi-objective optimization evolutionary algorithm, called NSGA-II, has implemented to identify the set of optimal solutions in MATLAB platform [7], in which minimizing the LCC, while maximizing the resilience index. Fig. 1 illustrates the flowchart of optimization framework procedure of this study.

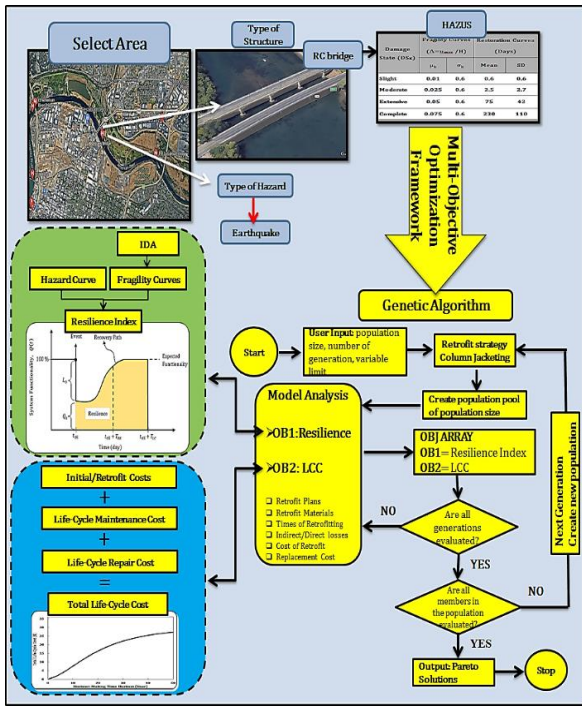


Fig. 1. An overall picture of multi-objective optimization process of this study

Background theories for resilience

In general, resilience $R(t)$ demonstrates the ability of infrastructure to sustain and recover to pre-event performance under hazard event, which can be determined by predefined level of functionality $Q(t)$ within a control time (T_{LC}) [8]. Mathematically, the resilience index can be defined as

$$R(t) = \int_{t_{0E}}^{t_{0E}+T_{LC}} \frac{Q(t)}{T_{LC}} dt \quad (1)$$

To the system functionality $Q(t)$, it is necessary to formulate two parameters of loss and recovery functions during the period of interruption as follows

$$Q(t) = 100\% - [L(I, T_{RE}) \times \{H(t - t_{0E}) - H(t - (t_{0E} + T_{RE}))\} \times f_{rec}(t, t_{0E}, T_{RE})] \quad (2)$$

in which $L(I, T_{RE})$ demonstrates the loss function as a function of hazard intensity (I) and elapsed time to recover (T_{RE}). In addition, f_{rec} and $H(\cdot)$ indicate the post-event recovery path and the Heaviside step functions of infrastructure, respectively. The system functionality (Q_0) or resilience index (R_0) after any event (t_{0E}) can be calculated in terms of a dimensionless cost as $\left(\frac{\text{Cost of repair}}{\text{Replacement cost}}\right)$ based on following relationship

$$R_0(\%) = Q_0 = 100\% - \sum_k P_E(LS_k) \cdot r_k \quad (3)$$

where $P_E(LS_k)$ implies the k th structural limit state which can be obtained from fragility curves, and r_k is derived in accordance with HAZUS [9].

Background theories for fragility curves

The fragility curves represent the probability of exceedance of each damage state (i.e., slight, moderate, extensive, and complete as the k th damage state; DS_k) for a wide range of ground motion Intensity Measure (IM) levels. In this study, the Maximum Drift (MD) and Peak Ground Acceleration (PGA) are considered as Engineering Demand Parameter (EDP) and IM indices for their efficiency, sufficiency and more practically in seismic vulnerability assessment, respectively [10]. The conditional probability $P_E(\cdot | \cdot)$ of demand being greater than the capacity can be analytically calculated as

$$P_E(D \geq DS_k | IM) = \phi \left[\frac{1}{\sigma_k} \ln \left(\frac{EDP}{\mu_k} \right) \right] \quad (4)$$

where $\phi[\cdot]$ is the log-normal cumulative distribution function with median (μ_k) and log-standard deviation (σ_k) as the input fragility parameters for each damage state in which are chosen based on HAZUS [9] (Table 1).

Table 1. Threshold of damage state quantities prescribed by HAZUS [9] for the case of initial intact state

Damage State (DS_k)	Fragility curves		Restoration curves (Days)	
	μ_k	σ_k	Mean	SD
Slight	0.01	0.6	0.6	0.6
Moderate	0.025	0.6	2.5	2.7
Extensive	0.05	0.6	75	42
Complete	0.075	0.6	230	110

Life-cycle cost analysis framework

The total life-cycle cost represents the risk of severe events in the form of financial losses during the service lifetime of the infrastructure [11]. The total incurred cost (C_T) generally include initial construction costs (C_0) total maintenance costs (C_M) and all costs incurred by users, agencies, economy and environment due to extreme hazards occurring during the lifetime of these structures (C_R). Additionally, in order to compare and calculate the discounted costs in different years, the Net Present Value

(NPV) of the expected value of costs is used in the LCC formulation as follow

$$\bar{C}_{R,NPT} = \bar{C}_0 + \bar{C}_{M,NPT} + \bar{C}_{R,NPT} \quad (5)$$

where $\bar{C}_{R,t}$ is the expected repair cost incurred at year t , which are considered as the expected sum of repair costs incurred during $[t, t + 1]$. Applying the total probability theorem, $\bar{C}_{R,t}$, is given by

$$\bar{C}_{R,t} = \sum_{n=1}^{N_{LS}} \bar{C}_r(LS_k) \times P(LS_k, [t, t + 1]) \quad (6)$$

where $\bar{C}_r(LS_k)$ is the expected repair cost when the infrastructure experiences limit state k , and $P(LS_k, [t, t + 1])$ is the probability of the structure sustaining limit state k between time t and $t+1$. The term $\bar{C}_r(LS_k) \times P(LS_k, [t, t + 1])$ in Eq. (6) is also called the risk cost of being at limit state k . Theoretically, if n incidents occur, the accumulated repair cost is the sum of the expected repair costs of sustaining limit state k times the probability of sustaining that damage state after each of such n hazard events. Consequently, the accumulated risk cost within period $[0, t]$ can be calculated as

$$\begin{aligned} & \bar{C}_{rp}(LS_k) \cdot P_E(LS_k, [0, t]) \\ &= \sum_{n=1}^{\infty} P_{nt}(n, t) \left(\sum_{j=1}^n \{ \bar{C}_{rp}(LS_k) \cdot P_E(LS_k^j | n, t) \} \right) \end{aligned} \quad (7)$$

where $P_{nt}(n, t)$ is the probability that n hazards occur during $[0, t]$ that can be calculated using the Poisson distribution function, and $P(LS_k^j | n, t)$ is the probability that limit state k is experienced by the infrastructure at j th hazard incident if n hazards take place during $[0, t]$. Noticeably, it is through this term, $P(LS_k^j | n, t)$, that the likelihood of incomplete repairs and consequently accumulation of damage are accounted. As mentioned, MD thresholds for bridge piers are considered to define slight, moderate, extensive, and complete damage as 1–4 seismic damage states, respectively. Consequently, for one type of damage and two consecutive damage states, the probability of being at the limit state between damage state k and $k + 1$ can be expressed as follows

$$P_E(LS_k) = P_E(DS_k) - P_E(DS_{k+1}) \quad (8)$$

Logically, repair actions are applied to damaged structure to return it to its original (intact) state. On the other hand, if the process of repairing damaged elements remains incomplete at the time of the hazardous event, in this case, it is assumed that the damage situation of the system is exactly equal to its state just before commencement of the repair actions. By applying the law of conditional probability, $P(DS_k^j | n, t)$ for a single hazard type can be calculated by

$$\begin{aligned} & P_E(DS_k^j | n, t) \\ &= \sum_{k'=1}^{N_{LS}} \sum_{RS} P_E(DS_k^j | [RS_{k'}, LS^{j-1}_{k'}], IM, n, t) \\ & \quad \cdot P([RS_{k'} | LS^{j-1}_{k'}], IM, n, t) \\ & \quad \cdot P_E([LS^{j-1}_{k'} | n, t]) \cdot P(IM) \end{aligned} \quad (9)$$

The probability of a specified intensity of hazard, $P(IM)$, can be evaluated using the hazard curve. Term $P(IM)$ can

be stated as $\frac{1}{v} \cdot |\Delta\lambda(IM)|$, which $\Delta\lambda(IM)$ indicates the exceedance rate of IM of the hazard. As discussed, term $RS_{k'}$ in Eq. (9) is the repair status that indicates whether the infrastructure system, after the $(j - 1)$ th hazardous event has been recovered ($RS_{k'} = 1$) or not ($RS_{k'} = 0$). Using the Bayes' theorem, the last term of the right side of Eq. (9) can be written as follow

$$\begin{aligned} & P([RS_{k'} = 0 | LS^{j-1}_{k'}, n, t]) \\ &= \frac{P([RS_{k'} = 0, n, t | LS^{j-1}_{k'}])}{P_{nt}(n, t)} \end{aligned} \quad (10)$$

The repair actions will be incomplete when structure is at limit state k' after the $(j - 1)$ th hazardous event, if the time difference between the $(j - 1)$ th and j th hazardous events is less than the required time to repair limit state k' (i.e., $\tau_{k'}$). In order to fulfil the condition of incomplete repair actions, no hazardous event should occur between the times t_{j-1} and t_j , (namely, $\{0, [t_{j-1}, t_j]\}$) that can simply write

$$\begin{aligned} & P([RS_{k'} = 0, n, t | LS^{j-1}_{k'}]) \\ &= \int_0^t \int_{t_{j-1}}^{\min\{t_{j-1} + \tau_{k'}, t\}} P(j \\ & \quad - 2, [0, t_{j-1}]) \cdot P(0, [t_{j-1}, t_j]) \cdot P(r \\ & \quad - j, [t_j, t]) \cdot v^2 \cdot dt_j \cdot dt_{j-1} \end{aligned} \quad (11)$$

As illustrated in the LCC computational framework, one of the most fundamental parameters in this framework is the fragility curves. It was primarily assumed that either the condition of the structure is in intact state, or the repair actions process has been completed before the j th hazardous event. Because of the lack of appropriate data, the ratios of the median of damage states for both cases of intact and damaged structures are obtained from Table 2. Also, the repair time of the case study structure is considered according to HAZUS [9] for four damage states (Table 1).

Table 2. The median of the fragility curves when the structure is intact to not initially in the intact state [9, 12]

Damage state in intact state	Damage state in fragility curve for initial below limit state			
	Slight		Moderate	
	E		C	
Moderate	1.25	E	E	
Extensive		1.25	C	C
Complete			1.25	2

In the multi-objective optimization process, one of the objectives is to minimize the LCC. In this study, the unit costs of the CFRP and GFRP are obtained \$105.92 and \$31.65/m², respectively. The average replacement cost for under-study bridge is about \$1833/m² [13], and the annual maintenance cost can be assessed as 0.5% of the structure replacement cost for all years. Additionally, the discount rate (r) has been estimated as 5%. In this study, the following costs are considered including (I) costs of repairing due to induced structural damage, (II) costs of delay time, vehicle operation, and excess gas emission on users, (III) cost of economic losses, (IV) cost of

environmental damage, and (V) cost of human casualties. It should be noted that these costs are added together to evaluate the total LCC, $\bar{C}_{rp}(LS_k)$ in Eq. (7). For more scientific basis and detailed discussion, refer to [11].

Modelling of illustrative case study

The considered RC box girder bridge is adopted per the bridge model presented by Sultan and Kawashima [14]. This bridge is assumed to be a three-lane with five-span (two 39.6 m exterior spans and three 53.3 m interior spans). Fig. 2 demonstrates more details on the structure modeled in the Finite Element (FE) SeismoStruct software [15]. For the purpose of pier retrofitting, the piers are jacketed with 2, 4, 7, and 10 plies (T1 to T4) of CFRP and GFRP with 1.24mm and 1.27mm thicknesses for each ply, respectively. The specifications of the materials considered in accordance with Omidian and Khaji [5] research. Additionally, eight different arrangements of the piers of the bridge are considered for the retrofit designs (Fig. 3).

This study uses the well-known nonlinear time-history IDA to produce the fragility curves for calculating seismic resilience. One of the key factors in the nonlinear dynamic analysis of structures is the selection of a minimum number of appropriate records because the results of the analyses are significantly dependent on the input ground motion. Hence, 20 time-histories are employed from the PEER [16]. Following, each record is scaled into 10 stages of from PGA=0.1g to 1g by incremental step of 0.1g. In addition, an earthquake with a return period of 475 years is used to exclusively calculate the resilience index which results PGA=0.4g based on the Probabilistic Seismic Hazard Analysis (PSHA) of under-study site.

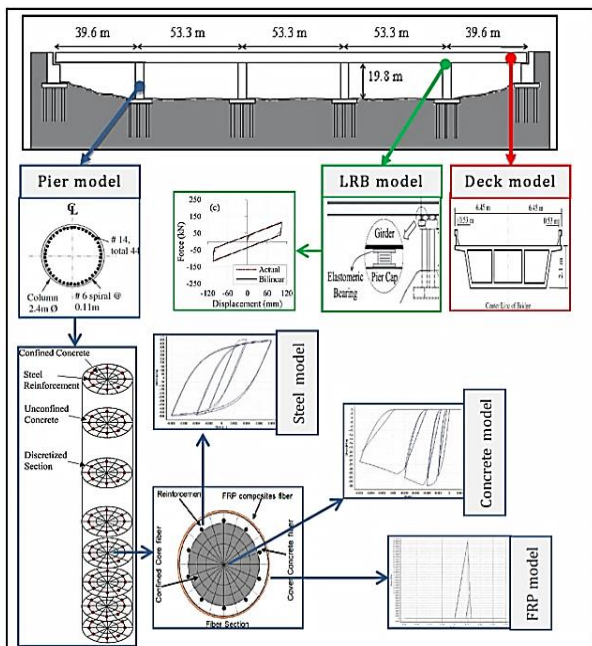


Fig. 2. Model specifications of considered bridge

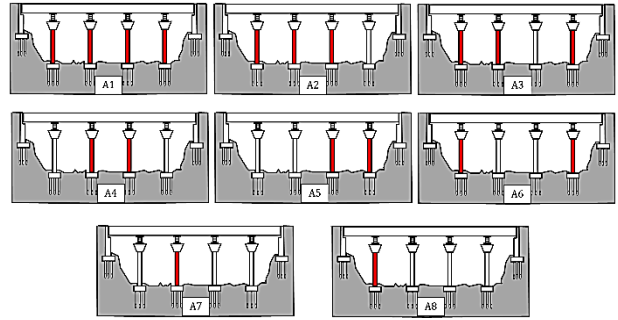


Fig. 3. Various arrangements used for bridge pier retrofitting

Results and discussion

The optimization is an organized process in order to find the best possible solutions for the multi-objective problems. In this study, different optimization objectives are examined in the form Multi-Objective Optimizations (MOO) by utilizing NSGA-II (see Fig. 1). In this regard, the under-study optimization problem minimizing the LCC and maximizing resilience index. The basic concept of optimization problem of the present study is formulated as presented in Table 3.

Table 3. The main steps of the NSGA-II

Initialize	
User input: population size (N_p), random initial population ($P_t \subset S$), number of generations t_{max} , variable limit	
Retrofit design: Arrangements (a : Various plans used for retrofitting configurations) & Materials (m : Steel, CFRP, GFRP) & Jacket thickness: (j : Steel jacketing: 9.53, 12.7, 19.05, 25.40mm CFRP jacketing: 2, 4, 7, 10 PLY (each ply=1.24mm) GFRP jacketing: 2, 4, 7, 10 PLY (each ply=1.27mm)) & Time of retrofitting: (tt : Various time of retrofitting used for LCC)	
Start	
While ($t < t_{max}$) do	
Generate offspring (Q_t)	
Mutate on Q_t	
Set $R_t = P_t \cup Q_t$	
Evaluate objective functions:	Resilience index (a, m, j) Life-cycle cost (a, m, j, tt) (or Cost of retrofit (a, m, j))
Apply non-dominated sorting on R_t :	Maximize: Resilience Index Minimize: Life-cycle cost (or Cost of retrofit)
Next generation:	Best of R_t population
End while	
Return the best set of solutions (Pareto Front)	
End	

Fragility and resilience curves

The concept of fragility curve can be used to quantify the seismic vulnerability of a system such as a bridge. In the following, the probability of four damage states is computed for a wide range of seismic intensity levels of 0 to 1g by assuming a log-normal distribution function (Fig. 4 (a-b)). The results show that the difference between the fragility values of each considered case is mainly varies based on the structural parameters such as different retrofit design, and site-specific seismic hazard parameter including seismic intensity level.

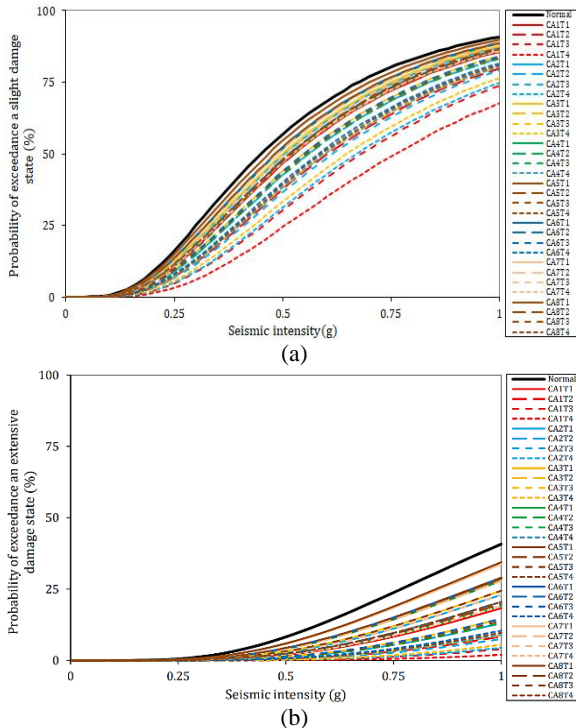


Fig. 4. Fragility curves for CFRP jacketing at the (a) slight, and (b) extensive damage state

The resilience can be calculated based on fragility curves and recovery functions. The resilience curve indicates the seismic resilience value right after an earthquake with different intensities (Fig. 5 (a)), and the resilience surface shows how the infrastructure recovers to its intact condition due to repairs (Fig. 5 (b)). It is observed that proper retrofit design makes the infrastructure less sensitive to destructive factors.

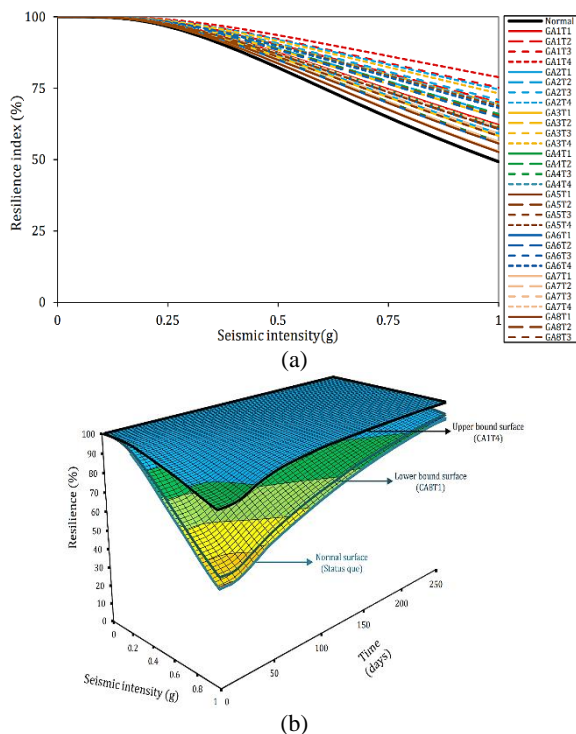


Fig. 5. Resilience curves for (a) GFRP jacketing, and (b) upper- and lower bounds of resilience surfaces for CFRP

Total life-cycle cost analysis

Total life-cycle maintenance cost

The total life-cycle maintenance cost is estimated only based on the worth of the structure as formulated, which includes the sum of initial value (or construction cost) and cost of retrofit (if it is retrofitted). As evidenced, the increase in this cost is correlated on how much more material (T1 to T4) and pier jacketing (A8 to A1) is used compared to the non-retrofitted structure that is the lowermost curve indicated by black dash line. In order to better and more comprehensively examine this point, the R/N ratio is suggested in which R and N are corresponded to the total life-cycle maintenance cost of the retrofitted and non-retrofitted structures, respectively Fig. 6.

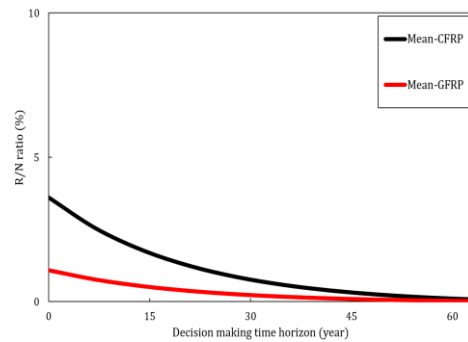


Fig. 6. The R/N ratio mean values of maintenance cost

Total life-cycle repair cost

The total life-cycle repair cost is the most important parameter in the total LCC estimation, where are included direct losses due to structural damage and indirect losses by the reason of agency, economic, environmental, human casualties, and user losses. As may be concluded from Fig. 7, the total life-cycle repair cost can change based on the two factors of hazard and fragility curves which are the outputs of site hazard characteristics and structural dynamic properties, respectively. In addition, different times of retrofitting can play striking role in reducing/increasing this cost. To further comparison, the Retrofit Efficiency (RE) ratio is used in which is the ratio of “useful output” to “total input” for the total life-cycle repair cost. In this formula, the useful output is equal to the amount of reduction in the total life-cycle repair cost due to retrofitting compared to the non-retrofitted structure, and the total input is equal to the total life-cycle repair cost of non-retrofitted structure.

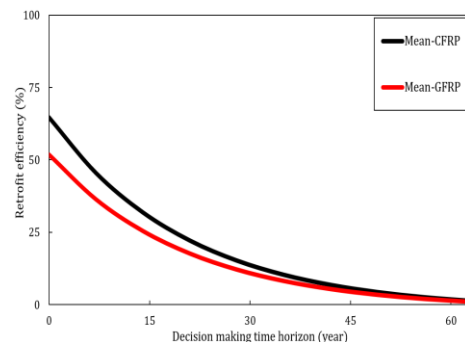


Fig. 7. The R/N ratio mean values of repair cost

Total life-cycle cost optimization

In order to fully calculate the total life-cycle cost, the total cost of retrofit should be added to the summation of the two terms of total life-cycle maintenance and repair costs as the Heaviside function in the considered year for retrofitting action. In this respect, the LCC is calculated for each retrofit design and shown in Fig. 8. The results indicate that the implementation of any retrofit design does not necessarily stand for reducing or optimizing the LCC during its life-cycle compared to the non-retrofitted situation. Besides, the time of retrofitting in combination with other retrofit design variables has an undeniable effect on decreasing or increasing the LCC (Fig. 8 (a–b)). Similar to the previous argument, the RE ratio is used for the LCC in order to better scrutinize the results of this section where positive and negative RE ratio indicate decreases and increase in the LCC, respectively (Fig. 8 (c)).

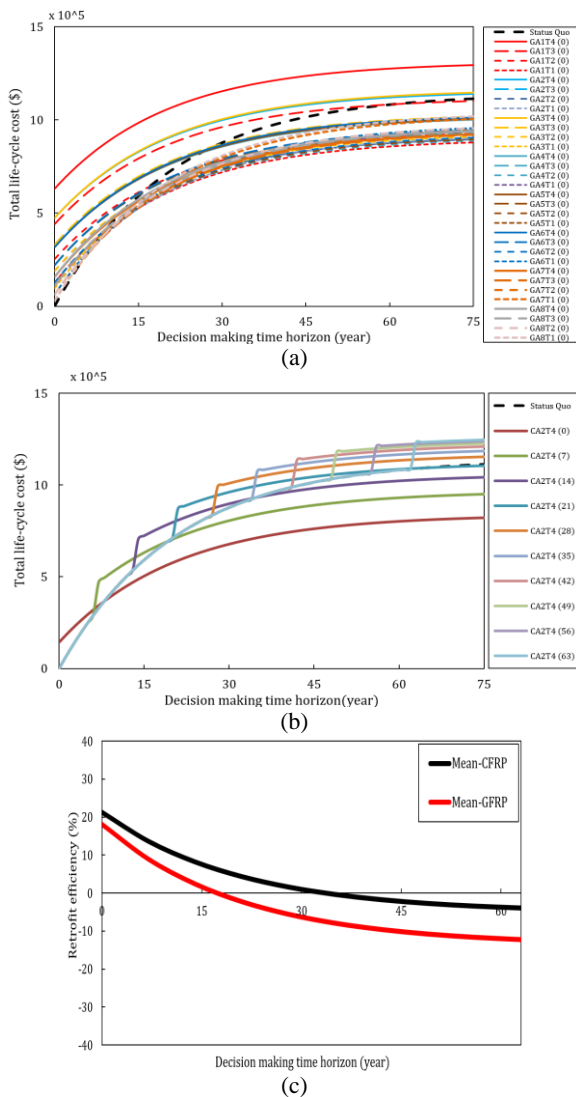


Fig. 8. The total life-cycle cost for (a) GFRP jacketing, (b) CA2T4 strategy at different times of retrofitting, and (c) RE mean values of LCC

The results demonstrate that in order to achieve the best retrofit strategies, a balance should be struck between the

two parameters of reducing the total life-cycle repair cost due to retrofitting and the cost of retrofit.

Multi-objective optimization

Financial and economic issues in civil infrastructure management and maintenance play a dominant role in choosing the right approach to select the optimal retrofit strategies. As a further critical matter, resilience index is essential in critical infrastructure sector to describe the level of performance for decision-makers. For this reason, a multi-objective optimization frameworks is presented and then determined for all under-study retrofit strategies. The suitability of each optimal set of solutions for different retrofit strategies is evaluated according to mentioned multi-criteria optimization including (1) minimizing the LCC and maximizing resilience index (as depicts in Fig. 9). In this regard, the most optimal retrofit strategies are presented in Table 4.

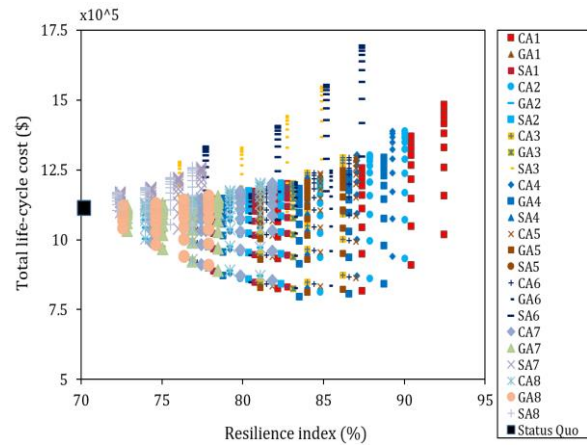


Fig. 9. The resilience index versus LCC for different retrofit strategies

Table 4. The most optimal retrofit strategies based on the LCC-resilience index objectives

No.	LCC-R		
	Strategy name	LCC (\$)	Resilience (%)
1	GA1T2 (0)	795534.8	83.5
2	GA1T3 (0)	806494.2	86.6
3	CA1T2 (0)	815736.1	87.4
4	GA1T4 (0)	841244.7	88.8
5	CA1T3 (0)	908594.5	90.4
6	CA1T4 (0)	1017805	92.5

The output results of multi-objective optimizations reveal that the most optimal retrofit strategies include jacketing all of the bridge piers with mid- to high- thickness of CFEP and GFRP in first years of retrofitting program, because the functionality/performance and cost-benefit effects are simultaneously and directly considered in this framework.

Conclusion

In this study, a sense-making optimization framework is proposed in the field of infrastructure management for

decision-making to prepare the most optimal retrofit strategies. For this purpose, a typical bridge is considered a case study infrastructure. The most optimal retrofit strategies are presented and discussed for under-study optimization approaches (i.e., resilience-LCC) by considering multiple retrofit strategies including different materials, thicknesses, arrangements and times of retrofitting actions. Specific conclusions of this research based on the obtained results are summarized as follows:

- The fragility curves are uniquely constructed based on the structural and site characteristics including retrofit designs and seismic input loads, respectively.
- The resilience curves/surfaces indicate that selecting a suitable retrofit design for the under-study infrastructure leads to less sensitive to destructive factors.
- The total life-cycle maintenance cost is only correlated on the sum of initial value (or construction cost) and cost of retrofit. According to the R/N ratio, this cost increases with the average of about 3% due to retrofit actions.
- The total life-cycle repair cost is changed based on the factors of site hazard characteristics, structural dynamic properties, and direct and indirect losses. Additionally, the time of retrofitting (as a key parameter in retrofit strategy) has outstanding effect in reducing repair costs.
- The output results of the total life-cycle cost demonstrate that each retrofit strategy has a different management on reducing or increasing the LCC compared to the non-retrofitted structure. In this respect, applying retrofitting actions in the first years has its maximum effect. In addition, in order to achieve the best retrofit strategy based on LCC criterion, a balance should be struck between the two key parameters of reducing the total life-cycle repair cost due to retrofitting and the cost of retrofit.
- In the end, a multi-objective optimization framework is proposed to find the most optimal retrofit strategies that maximizes the resilience index, while minimizes the LCC. The proposed LCC-resilience approach eliminates more inappropriate strategies, because the the level of functionality and cost-benefit are simultaneously and directly considered in this approach.

References

- [1] Y. Dang, Ch. Yan, and P. Niu. "Hysteretic model of reinforced concrete bridge piers based on earthquake damage and corrosion from saline soil," *Soil Dynamics and Earthquake Engineering*, 166, Article 107732, 2023. DOI:10.1016/j.soildyn.2022.107732
- [2] Z. Wang, D.Y. Yang, D.M. Frangopol, and W. Jin. "Inclusion of environmental impacts in life-cycle cost analysis of bridge structures," *Sustainable and Resilient Infrastructure*, 5(4), 252-267, 2020. DOI: 10.1080/23789689.2018.1542212
- [3] N.L. Dehghani, E. Fereshtehnejad, and A. Shafieezadeh. "A Markovian approach to infrastructure life-cycle analysis: Modeling the interplay of hazard effects and recovery," *Earthquake Engineering and Structural Dynamics*, 50(3), 736-755, 2020. DOI:10.1002/eqe.3359
- [4] J. Zhu, and B. Liu. "Performance life cost-based maintenance strategy optimization for reinforced concrete girder bridges," *Journal of Bridge Engineering*, 18(2), 172-178, 2013. DOI:10.1061/(ASCE)BE.1943-5592.0000344
- [5] P. Omidian, and N. Khaji. "A multi-objective optimization framework for seismic resilience enhancement of typical existing RC buildings," *Journal of Building Engineering*, 52, Article 104361, 2022. DOI:10.1016/j.job.2022.104361
- [6] A. Abarca, R. Monteiro, and G.J. O'Reilly. "Exposure knowledge impact on regional seismic risk assessment of bridge portfolios," *Bulletin of Earthquake Engineering*, 20, 7137-7159, 2022. DOI:10.1007/s10518-022-01491-z
- [7] K. Deb, A. Prata, A. Agarwal, and T. Meyarivan. "A fast and elitist multi-objective genetic algorithm: NSGA-II," *IEEE Transactions on Evolutionary Computation*, 6, 182-197, 2002.
- [8] Y. Zhang, J.F. Fung, K.J. Johnson, and S. Sattar. "Review of Seismic Risk Mitigation Policies in Earthquake-Prone Countries: Lessons for Earthquake Resilience in the United States," *Journal of Earthquake Engineering*, 26(12), 6208-6235, 2021. DOI:10.1080/13632469.2021.1911889
- [9] HAZUS-MH MR5. "Multi-hazard loss estimation methodology-earthquake model," Department of Homeland Security", Washington DC, 2014.
- [10] J.M. Patel, and J. Ghosh. "Influence of vehicular movement on the seismic response and fragility of highway bridge structures," *Structure and Infrastructure Engineering*, 2023. DOI:10.1080/15732479.2023.2165691
- [11] H. Fereshtehnejad, and A. Shafieezadeh. "A multi-type multi-occurrence hazard lifecycle cost analysis framework for infrastructure management decision making," *Engineering Structures*, 167, 504-517, 2018. DOI:10.1016/j.engstruct.2018.04.049
- [12] M. Raghunandan, A.B. Liel, and N. Luco. "Aftershock collapse vulnerability assessment of reinforced concrete frame structures," *Earthquake Engineering and Structural Dynamics*, 44(3), 419-439, 2015. DOI:10.1002/eqe.2478
- [13] Caltrans. Historic bridge inventory, sample plans of actions. Division of Maintenance, Structure Maintenance, 2005.
- [14] M. Sultan, and K. Kawashima. Comparison of the seismic design of highway bridges in California and in Japan, Recent selected publications of Earthquake Engineering Div., Public Works Research Institute (PWRI), Japan, 1993 (Technical Memorandum of PWRI No. 3276).
- [15] SeismoStruct. SeismoSoft, A computer program for static and dynamic nonlinear analysis of framed structures, 2023.
- [16] PEER. Pacific Earthquake Engineering Research center, online strong motion database, 2023.